

Numerical study of laser-induced surface acoustic waves in different thickness pipes

Yuejuan He (何跃娟)^{1,3}, Rihong Zhu (朱日宏)¹, Zhonghua Shen (沈中华)²,
 Jian Lu (陆建)², and Xiaowu Ni (倪晓武)²

¹ College of Electronic Engineering & Photoelectric Technology;

² College of Science, Nanjing University of Science & Technology, Nanjing 210094

³ College of Science, Southern Yangtze University, Wuxi 214062

The surface acoustic waves generated by a pulsed laser in pipes are studied by using the finite element method. The time domain waveforms of guided waves in three different thickness pipes are obtained in the near field. The numerical results denoted that the excited waves by a pulsed laser in a thin-walled pipe are typical lamb wave like in a thin plate, while in a thick pipe the main features of the surface waves are two kinds of waves: the surface skimming longitudinal wave and the Rayleigh wave, which will be useful in the applications in non-destructive evaluation of pipes.

OCIS codes: 140.0140, 140.6810, 170.7170.

Excitation of thermo-elastic waves by a pulsed laser in solid has attracted more and more attention owing to its wide applications in non-destructive evaluation and characterization of materials. A large amount of work has been devoted to solving the thermo-elastic wave problems^[1-4], but all of these works are dealing with the plate. It is very important to pay attention to the nondestructive detection of hollow cylinders because hollow cylinders are often used with the development of the industry. In the nondestructive detection of hollow cylinders, most of previous works^[5-7] are the application of using ultrasonic waves produced by machines which can exchange other kinds of energy to ultrasound. But ultrasound generated by pulsed laser is more convenient because laser-ulasonics need not to touch the sample during the detection. There are some works on laser-induced ultrasound in pipes but they only concentrate their attention on the experiment^[8,9].

Due to the complexity of the laser-matter interaction, numerical methods will be much more suitable in dealing with complicated processes, especially in dealing with the processes involving varied parameters. The finite element method, adopted in this paper, has many advantages^[10]. The finite element method is versatile due to its flexibility in modeling complicated geometry and its capability in obtaining full field numerical solution. So in this paper, based on thermo-elastic theory and considering the temperature-dependence of the thermal physical parameters of the material, we use the finite element method to analyze the surface acoustic waves in the circumferential direction of the pipe.

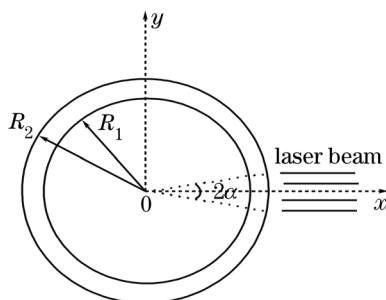


Fig. 1. Schematic diagram.

The geometry of laser irradiation on a hollow cylinder is shown in Fig. 1. It consists of a linear elastic, homogeneous, isotropic hollow cylinder with inner radius R_1 and outer radius R_2 . Here we assume that there is irradiation of laser beams in all the axial direction of the pipe.

Because we only concentrate our attention on the circumferential guided waves in this paper, so a two-dimensional (2D) cylindrical coordinate system is adopted, and the thermal conductive equation can be described as

$$\rho c \frac{\partial T(r, \phi, t)}{\partial t} - \kappa \left(\frac{\partial^2}{\partial r^2} T(r, \phi, t) + \frac{1}{r} \frac{\partial}{\partial r} T(r, \phi, t) + \frac{1}{r^2} \frac{\partial^2}{\partial \phi^2} T(r, \phi, t) \right) = 0, \quad (1)$$

where $T(r, \phi, t)$ represents the temperature distribution at time t , ρ , c and κ are the density, thermal capacity and thermal conductive coefficient, respectively.

The laser irradiation is considered to serve as a surface heat source and the inner surface of the hollow cylinder is supposed to be thermal insulation, so that the boundary conditions at these two surfaces can be written as

$$\begin{cases} -\kappa \frac{\partial T(r, \phi, t)}{\partial r} \Big|_{r=R_2, -\alpha \leq \phi \leq \alpha} = P(1 - R) \\ -\kappa \frac{\partial T(r, \phi, t)}{\partial r} \Big|_{r=R_2, \alpha < \phi < \pi} = 0 \\ -\kappa \frac{\partial T(r, \phi, t)}{\partial r} \Big|_{r=R_2, -\pi < \phi < -\alpha} = 0 \end{cases}, \quad (2)$$

and

$$-\kappa \frac{\partial T(r, \phi, t)}{\partial r} \Big|_{r=R_1} = 0, \quad (3)$$

where R is the reflectivity of the film surface, $[-\alpha, \alpha]$ is the range of laser irradiation in the outer surface of the pipe, P is the laser power density, which can be described as

$$P = P_0 g(t), \quad (4)$$

where P_0 is the peak power density and $g(t)$ is the temporal distribution of the laser pulse. The function form can be written as

$$g(t) = \frac{t}{t_0} e^{-\frac{t}{t_0}}, \quad (5)$$

where t_0 is the rise time of the laser pulse. And we consider the spatial distribution of the laser pulse is uniform. The initial condition for the temperature field is $T_0 = 300$ K.

The thermo-elastic wave equation is

$$(\lambda + 2\mu)\nabla(\nabla \cdot U) - \mu\nabla \times \nabla \times U - \alpha(3\lambda + 2\mu)\nabla T(r, \phi, t) = \rho \frac{\partial^2 U}{\partial t^2}, \quad (6)$$

with the initial conditions

$$U(r, \phi, t)|_{t=0} = \frac{\partial U(r, \phi, t)}{\partial t}|_{t=0} = 0, \quad (7)$$

where $U(r, \phi, t)$ is the transient displacement, λ and μ are the lame constants, and boundary condition is the outer surface and the inner surface are free.

Based on the theories described above, we have calculated the transient displacement fields in three different thickness pipes. In order to study the surface acoustic waves varying with the thickness of the pipe, we take the same outer radius R_2 as 15 mm and three different inner radius R_1 as 14.8, 14, and 10 mm. That is to say, the thicknesses in radial orientation of the pipes are 0.2, 1, and 5 mm. And we suppose that the length of the sample is 6 mm. The angular range of the laser irradiation in the outer surface of the pipes is $-0.5^\circ \leq \phi \leq 0.5^\circ$. That is to say, the beam of the laser spot is focused onto a about 260 μm -wide line. The laser energy is 100 mJ, and the pulse rise time t_0 is taken to be 10 ns. The reflectivity of the aluminum surface R is 0.9. The temperature dependence of thermal conductivities of aluminum can be expressed as

$$\kappa = \begin{cases} 249.45 - 0.085T, & 200 \leq T \leq 730 \\ 198.47 - 0.014T, & 730 < T < T_m \end{cases}, \quad (8)$$

where T is the temperature measured in Kelvin. The specific heat capacities of aluminum can be expressed as

$$c = 780.27 + 0.488T, 200 \leq T < T_m, \quad (9)$$

The densities of aluminum and polymethyl methacrylate can be expressed as

$$\rho = 2769 - 0.22T, 300 \leq T < T_m. \quad (10)$$

where T_m is the melting point of aluminum. The units of all the parameters referred above use standard units. And the mechanical properties of aluminum in the calculation are Young's modulus of 7.02×10^{10} Pa, Poisson's ratio of 0.34, thermal expansion coefficient of 2.31×10^{-5} K^{-1} , lame constants $\lambda = 5.81 \times 10^{10}$ Pa, and $\mu = 2.61 \times 10^7$ Pa. In our calculation, the maximum element size is arranged to be 100 μm , and considering that the rise time of the laser pulse is only 10 ns, we arranged the maximum time step of the finite element method to be 0.2 ns.

Figure 2 shows the time domain waveforms of the surface radial normalized displacement at the point of $\phi = 10^\circ$ in the outer surface and the inner surface of the 0.2 mm-walled pipe.

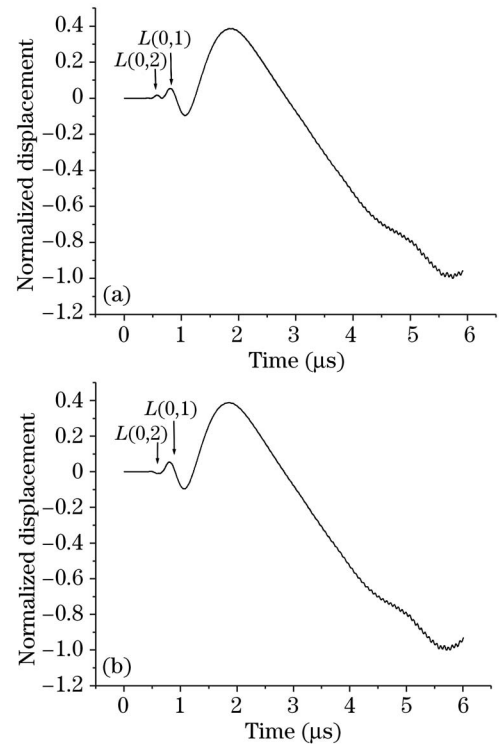


Fig. 2. Radial normalized displacement versus time at the point of source-receiver angle of 10° in the 0.2-mm-walled pipe. (a) Outer surface, (b) inner surface.

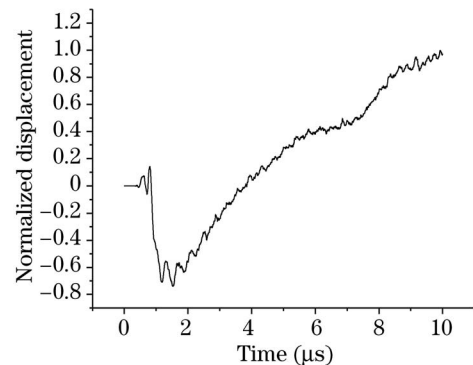


Fig. 3. Radial normalized displacement versus time at the point of source-receiver angle of 10° in the 1-mm-walled pipe.

From Fig. 2, it can be seen that the waves are typical lamb wave like in a thin plate. Compared the Figs.2(a) and (b), we know that the first wave is the symmetric $L(0,2)$ mode of the pipe's guided waves, which is corresponding to the S_0 mode in a thin plate. And the second wave is the anti-symmetric $L(0,1)$ mode, which is corresponding to the a_0 mode in a thin plate.

Figure 3 shows the time domain waveforms of the surface radial normalized displacement at the point of $\phi = 10^\circ$ in the 1-mm-walled pipe. In Fig.3, the waveforms gradually lose the form identifiable as that of a guided Lamb wave mode while increasing the pipe's thickness.

Figure 4 shows the time domain waveforms of the surface radial normalized displacement at the point of $\phi = 10^\circ$ in the 5-mm-walled pipe. From it, We can see

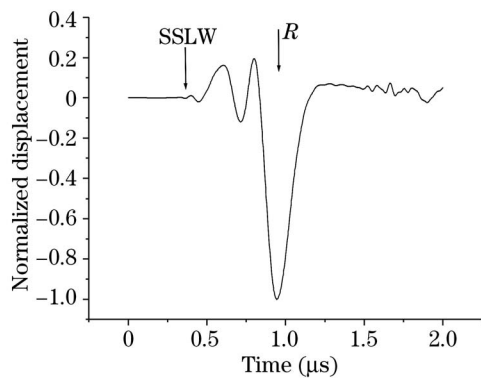


Fig. 4. Radial normalized displacement versus time at the point of source-receiver angle of 10° in the 5-mm-walled pipe.

that the main features of the surface waves are two kinds of waves. One is the surface skimming longitudinal wave denoted by SSLW, the other is the Rayleigh wave denoted by R in the Fig. 4. Because the propagating velocity of the SSLW is the largest, the amplitude of the Rayleigh wave is the most.

By using the finite element method, we obtain the surface radial normalized displacements fields generated by a pulsed laser in three different thickness pipes. The numerical results denoted that the excited waves by a pulsed laser in a thin-walled pipe are typical lamb wave like in a

thin plate, while in a thick pipe the main features of the surface waves are two kinds of waves: the surface skimming longitudinal wave and the Rayleigh wave, which will be useful in the applications in non-destructive evaluation of pipes.

Y. He's e-mail address is yuejuanhe@thmz.com.

References

1. A. F. McDonal, Appl. Phys. Lett. **56**, 230 (1990).
2. X. Wang and X. Xu, Appl. Phys. A **23**, 107 (2001).
3. Z. H. Shen and S. Y. Zhang, Micro. & Opt. Tech. Lett. **28**, 364 (2001).
4. B. Q. Xu, Z. H. Shen, J. Lu, X. W. Ni, and S. Y. Zhang, Int. J. Heat and Mass Transfer **46**, 4963 (2003).
5. D. N. Alleyne, M. Lowe, and P. Cawley, J. Appl. Mech. **65**, 635 (1998).
6. M. Lowe, D. N. Alleyne, P. Cawley, J. Appl. Mech. **65**, 649 (1998).
7. J. J. Ditre and J. L. Rose, J. Appl. Phys. **72**, 2589 (1992).
8. W. M. Gao, C. Glorieux, and J. Thoen, J. Appl. Phys. **91**, 5521 (2002).
9. D. Clorennec and D. Royer, Appl Phys Lett. **82**, 4608 (2003).
10. B. Q. Xu, Z. H. Shen, X. W. Ni, J. J. Wang, J. F. Guan, and J. Lu, J. Appl. Phys. **95**, 2116 (2004).